Theoretical investigation of native defects, impurities, and complexes in aluminum nitride

C. Stampfl[1] and C. G. Van de Walle[2]
[1]*Department of Physics and Astronomy, Northwestern University, Evanston, Illinois 60208-3112*
[2]*Xerox Palo Alto Research Center, 3333 Coyote Hill Road, Palo Alto, California 94304*
(Received 1 November 2001; published 15 April 2002)

We have performed density-functional pseudopotential calculations to investigate the electronic structure, atomic configurations, and formation energies of native point defects and impurities in AlN. For the native defects, the nitrogen vacancy has the lowest formation energy in *p*-type material and the aluminum vacancy has the lowest formation energy in *n*-type material. Under *n*-type conditions the formation energy of the nitrogen vacancy is high, indicating that it will not occur in high concentrations. We find that the nitrogen vacancy exhibits a *different* behavior in the zinc-blende and wurtzite structures with respect to the higher-lying defect-induced level: in zinc-blende materials, this level is a resonance in the conduction band causing the vacancy to act as a shallow donor, while in wurtzite the level lies well below the conduction-band edge causing the vacancy to act as a deep donor. In the zinc-blende structure we find, in addition, that the aluminum interstitial has a low formation energy in *p*-type material. The results indicate that these defects could be important compensation centers; we discuss this in relation to the dopant impurities O, Si, and Mg. We also investigate MgO and Mg_2O_2 impurity complexes. A comparison between results obtained using the local-density approximation and the generalized-gradient approximation for the exchange-correlation functional shows that the results are qualitatively very similar.

DOI: 10.1103/PhysRevB.65.155212 PACS number(s): 61.72.Ji, 71.15.Nc, 71.55.Eq

I. INTRODUCTION

Group-III nitride materials are being intensively researched due to their demonstrated success in optoelectronic devices and their further potential in this area.[1–3] For example, highly efficient blue and green light-emitting diodes have been fabricated,[4] and nitride-based laser diodes have been developed.[5,6] Considerable effort is being focused on obtaining an understanding of the microscopic electronic and atomic structure which will afford further improvement and control of device performance. An important step in this direction is the study of native point and impurity defects. While there have been several theoretical studies of point defects in GaN, less work has been done on AlN. It is, however, important to understand the behavior of defects in AlN in addition to GaN since, e.g., the cladding and confinement layers which surround the active region of a laser diode are typically $Al_xGa_{1-x}N$, for which it must be possible to perform both *n*- and *p*-type doping. Successful *p*- and *n*-type doping of AlN could also lead to important applications for this material. In GaN, one factor limiting *p*-type conductivity is self-compensation, apparently resulting from the formation of donor-acceptor pairs;[7,8] a similar problem could also occur for AlN, which to date has resisted attempts at doping.

With respect to theoretical studies of native defects and impurities in AlN, we mention the following: Jenkins and Dow[9] considered defects in the neutral charge state using an empirical tight-binding method. Defect levels were reported, but no calculation of formation energies was attempted. More recently, first-principles pseudopotential calculations were performed by Mattila and Nieminen,[10] who reported formation energies of various charge states of the N and Al vacancies and the O impurity in zinc-blende AlN, as well as the N antisite.[11] It was reported that the nitrogen vacancy (V_N) induced two states in the band gap, one doubly occupied state lying above the valence-band maximum (VBM) and a higher-lying level that could be occupied with one or three electrons (the neutral and singly negative charge states being unstable). The nature of the latter state is different from what was reported in our subsequent work (Refs. 12 and 13), where we found that the upper V_N-induced state was a resonance in the conduction band. As we explain below, it appears that the calculations of Ref. 10 erroneously occupied the lowest conduction band rather than the defect state. Recently, Fara *et al.*[14] studied Al and N vacancies as well as selected impurities in *wurtzite* AlN for various charge states using the pseudopotential method. With respect to the nitrogen vacancy, they found the upper defect state to be deep in the band gap, i.e., about 1–3 eV below the conduction-band minimum. Our systematic calculations will indeed confirm this difference between zinc-blende and wurtzite material, the nitrogen vacancy acting as a shallow donor in the former, but as a deep donor in the latter.

Regarding impurities, C, Si, and Ge (Ref. 15) and Si and Ge (Ref. 16) in wurtzite GaN and AlN were investigated in the neutral charge state by Boguslawski *et al.* and by Park and Chadi, respectively. Finally, Gorczyca *et al.*[17] investigated native point and impurity defects using the Green's-function technique based on the linear muffin-tin orbital method in the atomic sphere approximation with no atomic relaxations included; here the emphasis was on the influence of hydrostatic pressure on the defect levels with no formation energies being reported. In a later publication these authors studied native defects and the C, Zn, and Mg impurities in cubic (zinc-blende) AlN and GaN in the neutral charge state, this time taking atomic relaxation into account and reporting formation energies.[18] With respect to the study of Mg and O defect complexes, Gorczyca *et al.*[19] investigated Mg-O (and

 ©2002 The American Physical Society

Mg-V_N) structures in (cubic) GaN, and proposed that such complexes could play a role in self-compensation when attempting *p*-type doping, which could also have implications for AlN. In earlier work, Van de Walle *et al.*[20] reported a binding energy of 0.6 eV for the Mg-O complex in both (zinc-blende) GaN and AlN.

In the present paper we perform a systematic investigation of the electronic and atomic structure, as well as defect formation energies, of native point defects, selected impurities (Si, O, and Mg), and defect complexes MgO and Mg_2O_2 in AlN using first-principles pseudopotential calculations. Some of these results were briefly reported earlier.[12,13] The paper is organized as follows: In Sec. II we describe the calculation method and in Sec. III results for the native defects are presented. Section IV describes results for the impurities and defect complexes, and Sec. V contains the conclusion.

II. CALCULATION METHOD

The calculations are performed using density-functional theory (DFT) and the pseudopotential plane wave method.[21] We use the supercell approach, and employ a tight-binding initialization scheme for the electronic wave functions to improve convergence. Both the local-density approximation[22] (LDA) and the generalized-gradient approximation[23] (GGA) for the exchange-correlation functional are used. In the literature the GGA is considered as a possible alternative for an improved treatment of the exchange-correlation functional over the LDA, and was found to yield a better description of a number of physical properties.[24] To date, there have been very few defect calculations that employ the GGA. AlN can assume both the zinc-blende and wurtzite structures, the latter being the stable phase and the former being stabilized through epitaxial growth.[25] The majority of our calculations are performed using 32-atom zinc-blende supercells and an energy cutoff of 40 Ry with two special **k** points in the irreducible part of the Brillouin zone.[26] We also performed some calculations for nitrogen and aluminum vacancies, which are the dominant native defects, using 32- and 72-atom wurtzite supercells with two and three special **k** points in the Brillouin zone,[27] respectively; the results obtained with the larger cell were very similar to the 32-atom cell. The positions of the atoms around the defects are relaxed using a damped dynamics approach.[21] The pseudopotentials are created using the scheme of Troullier and Martins,[28] and for the GGA calculations we include the GGA in the creation of the pseudopotential as well as in the self-consistent total-energy calculations, so that the description is consistent.[29,30] In earlier work[31] we thoroughly tested the performance of these pseudopotentials, and found bulk properties in very good agreement with other available *ab initio* results. These potentials have also been used in our other recent studies of group-III-nitride systems.[12,13,32,33] While the GGA improved the properties for N_2, bulk Al, and AlN, the improvement for GaN was less significant and for InN, we found that the GGA exhibited an underbinding.

The formation energy of a native point defect in charge state q in AlN is expressed as

$$E^f(q)=E^{\rm tot}_{\rm defect}(q)-E^{\rm tot}({\rm bulk})-n_{\rm Al}\mu_{\rm Al}-n_{\rm N}\mu_{\rm N}+qE_F\,, \tag{1}$$

where $E^{\rm tot}_{\rm defect}(q)$ is the total energy of the supercell containing the defect, $E^{\rm tot}(\rm bulk)$ is the total energy of a similar supercell containing the pure bulk crystal, $n_{\rm Al}$ and $n_{\rm N}$ are the number of Al and N atoms, respectively, that are added to or taken from the bulk crystal in order to create the defect, and $\mu_{\rm Al}$ and $\mu_{\rm N}$ are the corresponding chemical potentials. E_F is the Fermi energy, which is set to zero at the valence-band maximum. We note that for charged defects, a proper lineup of the band structure of the defect supercell with that of the bulk is required. This is done using the difference in the average potential around an atom in a bulklike environment as a measure of the shift needed to line up the band structure (see Refs. 34 and 35 for details).

A low value of the formation energy indicates a high equilibrium concentration of defects, while a high value implies a low concentration. That is, for a given temperature and in the limit of low concentrations, one can assume that the defect concentrations obey an Arrhenius type of behavior, which means that the logarithms of the concentrations are proportional to the formation energies.

The chemical potentials depend on the experimental conditions under which the material is grown. In order to determine these quantities, we invoke the relationship $\mu_{\rm Al}+\mu_{\rm N}=\mu_{\rm AlN}$, assuming both species are in thermal equilibrium with AlN. Furthermore, the chemical potentials must satisfy the boundary conditions: $\mu_{\rm N}<1/2\mu_{\rm N_2}$ and $\mu_{\rm Al}<\mu_{\rm Al(bulk)}$ (if this were not the case, then AlN would be thermodynamically unstable with respect to the formation of N_2 molecules or bulk Al). When imposing certain growth conditions [nitrogen-rich ($\mu_{\rm N}=1/2\mu_{\rm N_2}$) or aluminum-rich ($\mu_{\rm Al}=\mu_{\rm Al(bulk)}$) conditions], the chemical potential for the other species can be determined from the above (thermal equilibrium) relationship.

For the case of an impurity of species X, a term $-n_X\mu_X$ will appear, in addition, on the right-hand side of Eq. (1). In the present work we consider O, Si, and Mg point impurities, and MgO and Mg_2O_2 defect complexes. The atomic chemical potentials are assumed to be determined by equilibrium with Al_2O_3, Si_3N_4, and Mg_3N_2 (leading to maximum solubility). For Al_2O_3 (sapphire) we use the calculated heat of formation of 18.4 eV (LDA) and 16.5 eV (GGA). To be consistent with the defect calculations, these values are obtained at the same energy cutoff, and we optimized the lattice constant. The experimental value is 17.24 eV.[36] For Si_3N_4 and Mg_3N_2 we use the experimental values of the heat of formation (4.81 and 7.70 eV, respectively[36]) together with the energy of the calculated elemental phase.

In the zinc-blende structure, AlN has an *indirect* band gap; we calculate the minimum gap (indirect $\Gamma_{15}-X_1$) to be 3.15 eV. The corresponding experimental value is not well established, but it will be notably larger than the theoretical one

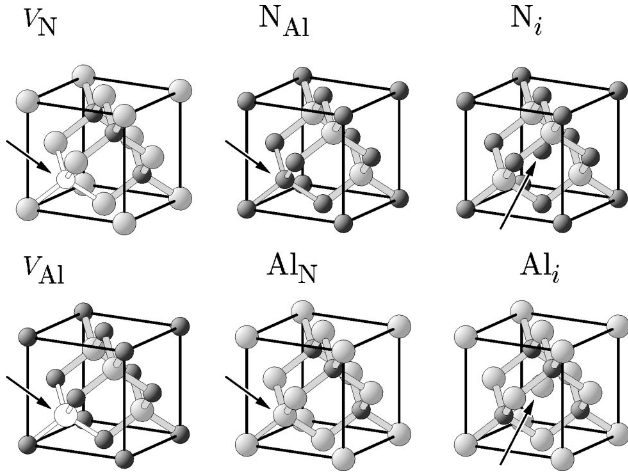

FIG. 1. Atomic geometry of native point defects in zinc-blende AlN in the ideal (unrelaxed) structure. Large gray and small dark spheres represent Al an N atoms, respectively. Vacancies are indicated by the white circles.

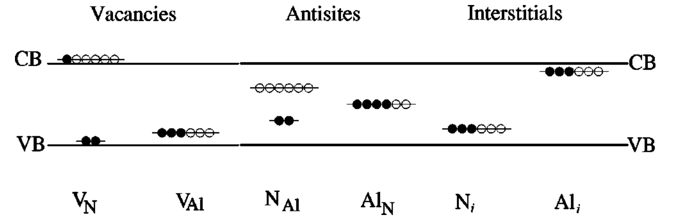

FIG. 2. Schematic representation of the defect-induced electronic states in zinc-blende AlN for the neutral charge state. Filled and open circles denote electrons and holes, respectively.

reported here due to the well-known tendency for DFT-LDA (and DFT-GGA) calculations (and even exact DFT (Ref. 37)] to underestimate band gaps. In the present work we consider E_F, spanning the indirect band gap of ≈ 5.0 eV as obtained from GW calculations.[38] The calculated wurtzite (direct) band gap is 4.74 eV, and the experimental value is 6.28 eV (see, e.g., Ref. 31).

III. NATIVE POINT DEFECTS

The ideal (unrelaxed) atomic geometry of the point defects in zinc-blende AlN is shown in Fig. 1: N and Al vacancies (V_N and V_{Al}), N and Al antisites (N_{Al} and Al_N), and N and Al interstitials (N_i and Al_i). The associated atomic relaxations are given in Table I. In the zinc-blende structure there are two interstitial sites with tetrahedral symmetry; one in which the interstitial atom is surrounded by four cations, and the other where it is surrounded by four anions. In Fig. 1 we only show the interstitial anion (cation) with cation (anion) nearest neighbors, since we found that these are the lower-energy defects. In the next subsections the associated defect electronic structure, formation energies, and atomic structure are discussed.

A. Electronic structure

In Fig. 2 the defect-induced Kohn-Sham levels are shown schematically for the neutral charge state in *zinc-blende* AlN. According to the present calculations, the nitrogen vacancy (V_N) introduces two states, an a_1 (s-like) state occupied by two electrons appearing above the valence-band maximum, and a triplet state t_2 (p-like) containing one electron, which is a resonance in the conduction band; the nitrogen vacancy thus acts as a single donor. (We keep in mind here that in the zinc-blende (ZB) structure, AlN has an indirect band gap, as noted earlier.) In the calculations, we find that the one electron associated with the t_2 state is located at the conduction-band edge and *not* in the defect level. Our calculated formation energy for the *neutral* charge state would therefore be unreliable (i.e., lower than it should be). Furthermore, within the DFT-LDA the band gap is notably smaller than experiment; corrections to the DFT-LDA would give rise to a larger band gap and also raise the formation energy of V_N^0. We can roughly estimate the formation energy of the nitrogen vacancy in the neutral charge state by approximating it to be the formation energy of the *positive* charge state when the Fermi level is at the bottom of the conduction band.[39] This

TABLE I. Defect geometries as a function of charge state for point defects and impurities in zinc-blende AlN. Displacements of the nearest-neighbor atoms are expressed as a percentage of the ideal bulk bond length. Positive values represent displacement away from the defect center, and negative values that toward it. For the N_{Al}^{EL2} defect, the values correspond to the percentage displacement of the N atom along the [111] direction with respect to the ideal N-Al distance, and for the N_i^{sp} defect, the values correspond to the percentage deviation in the distance between the two N atoms that share the substitutional site, referenced to the bond length of the N_2 molecule.

Charge state	V_N	V_{Al}	N_{Al}	N_{Al}^{EL2}	Al_N	N_i	N_i^{sp}	Al_i	Mg_{Al}	O_N	Si_{Al}
−3		9.2									
−2		9.7		38.8							
−1		9.7	7.5	45.2	17.3	−2.1	35.3		9.4		
0		10.5	0.9	48.9	19.0	0.5	24.8	−3.6	10.1		
1	2.3		8.2		21.0	3.1	15.4	−3.6		3.8	−5.0
2	9.1		15.4		23.4		9.3	−4.0			
3	17.3				25.9		4.8	−4.1			
4					28.5						

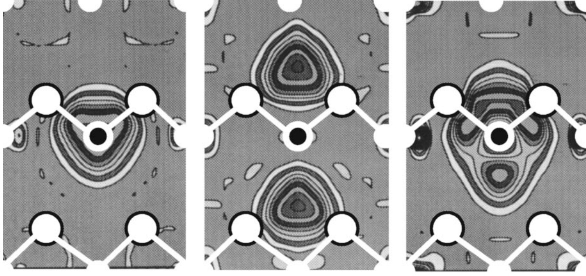

FIG. 3. Electron density distributions in the (110) plane of zinc-blende AlN for (left) the lower a_1-like nitrogen vacancy state, (center) the state at the conduction band minimum, and (right) the higher-lying t_2-like nitrogen vacancy state. Large and small white circles represent Al and N atoms, respectively, and the black dots indicate the nitrogen vacancy.

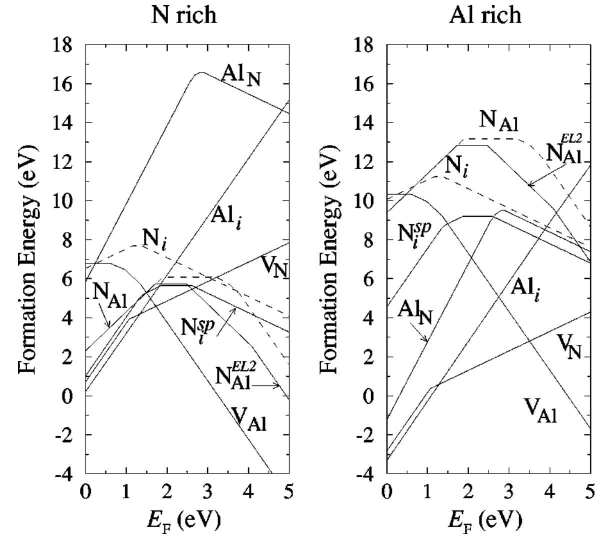

FIG. 4. Defect formation energies (LDA) for native point defects in zinc-blende AlN as a function of the Fermi level under nitrogen-rich (left panel) and aluminum-rich (right panel) conditions. $E_F=0$ corresponds to the valence-band maximum.

gives a value of about 7.8 eV for N-rich conditions, and one of about 4.3 eV for Al-rich conditions using the *GW* band gap[38] of 5.0 eV. We point out that attempts to occupy this upper defect level, i.e., considering negatively charged states (e.g., V_N^{1-}, V_N^{2-}, V_N^{3-}, etc.) will be unsuccessful, since, rather than the defect state, the conduction band will be occupied, leading to erroneous results. We believe that this was the case in Ref. 10.

The behavior of the nitrogen vacancy in *wurtzite* AlN is quite different. The band gap of wurtzite AlN is significantly larger than that of ZB AlN, and the upper defect state now lies *below* the conduction-band minimum. In order to confirm these assignments, we have performed calculations using self-interaction and relaxation-corrected (SIRC) pseudopotentials which afford an accurate description of the band gap:[40] for zinc-blende AlN we obtain a band gap of 5.05 eV (in very close agreement with the *GW* result) and for the wurtzite structure one of 6.50 eV. We have found that the t_2 nitrogen vacancy state is indeed *above* the conduction-band minimum in the zinc-blende structure and *below* it in the wurtzite structure. The calculations were carried out analogously to those reported in Ref. 33; further details will be given in a forthcoming publication.[41] In Ref. 33 we compared the position and nature of native defects in InN as obtained using the LDA and SIRC potentials, and found that the SIRC calculations affect the positions of some of the defect states in the band gap, but the general conclusions obtained from the standard DFT calculations remained valid. In Fig. 3, we show the spatial distribution (as obtained from our DFT-LDA calculations) of the (lower) a_1-like nitrogen defect state; the next highest state, which is an extended state at the conduction-band minimum (CBM); and the t_2-like nitrogen defect state, which is at an energy higher than the CBM state. The former and latter are clearly localized at the vacancy, while that at the CBM is a bulk state of Al character.

The aluminum vacancy (V_{Al}) creates a triplet state in the lower part of the band gap (see Fig. 2) which is occupied by three electrons and can be filled with three more electrons, i.e., V_{Al} is a triple acceptor. For the substitutional nitrogen antisite (N_{Al}) a doubly occupied singlet state in the band gap is introduced, as well as an empty triplet state higher in the band gap which can trap six electrons. Depending on the position of the Fermi level, N_{Al} may act as an acceptor or a donor (i.e., this defect, and the following two discussed, exhibit an amphoteric behavior). The aluminum antisite (Al_N) introduces a deep triplet level deep in the band gap. It is occupied by four electrons, and can be filled with two more electrons, or emptied of all four, thus acting either as an acceptor or a donor. For the tetrahedrally coordinated nitrogen interstitial (N_i), a triplet state in the band gap results, which is occupied by three electrons. This level can be filled by three more electrons or conversely emptied of three electrons, again acting respectively as an acceptor or donor depending on the position of the Fermi level. The aluminum interstitial (Al_i), finally, introduces a triplet state in the upper part of the band gap, occupied by three electrons (see Fig. 2), and is thus a triple donor. For the Al interstitial at the *O* site (see Fig. 5) in the wurtzite structure, which is lower in energy than the *T* site (as discussed below), there is a doubly occupied single deep donor level and a higher lying singlet level occupied by one electron.

B. Formation energy

In the left and right panels of Fig. 4 we present the calculated defect formation energies for the various charge states as a function of the Fermi energy E_F in zinc-blende AlN, for N- and Al-rich conditions, respectively. For clarity, for each charge state of each defect we have not plotted the full straight line, but show only the section where that charge state is lower in energy than all other charge states. Thus the change in slope of the lines represents a change in the charge state of the defect [cf. Eq. (1)]. We note that the difference in formation energies of the vacancies between N- and Al-rich conditions is exactly the heat of formation of AlN: $\Delta H = E_{AlN}^{tot} - E_{Al,bulk}^{tot} - 1/2 E_{N_2}^{tot}$, where E_{AlN}^{tot}, $E_{Al,bulk}^{tot}$, and $E_{N_2}^{tot}$ are

the total energies of bulk AlN, bulk Al, and the N_2 dimer, respectively. This is also the case for the interstitial defects, but here the difference is $-\Delta H$. The difference in formation energy between N- and Al-rich conditions for the antisites corresponds to twice the heat of formation. We calculate the heat of formation of AlN to be -3.40 and -3.05 eV for the LDA and GGA, respectively. The experimental value of ΔH is -3.28 eV.[25] Note that the negative formation energies occurring in Fig. 4 are not a problem; indeed, charge neutrality will constrain the Fermi level to a region where the formation energies are positive.

1. Vacancies

It can be seen that under *p*-type conditions (low E_F values) the nitrogen vacancy in the triply positively charged state, V_N^{3+}, has a very low formation energy. We find that the doubly positively charged nitrogen vacancy V_N^{2+} is unstable, thus presenting a negative-*U* effect between triply and singly positive charge states. This has also been found to occur in GaN.[16,42] The transition level $E^{3+/+}$ of V_N in AlN is about 1.0 eV, to be compared with ≈ 0.2 eV in GaN.[42] Our results for V_N^{+} and V_N^{2+} are in good agreement with the calculations of Mattila and Nieminen;[10] those authors, however, did not investigate V_N^{3+}. In positive charge states (cf. our discussion in Sec. III A), we expect the calculated formation energies to be accurate, since the one electron that was a resonance in the conduction band is removed.[43] Under *n*-type conditions we see that the formation energy of the nitrogen vacancy is high, indicating that this defect will not occur in high concentrations. Nitrogen vacancies were previously shown not to be a cause of *n*-type conductivity in GaN (Ref. 44); combined with the present results for AlN, we can conclude that nitrogen vacancies will also not be a cause of *n*-type conductivity in $Al_xGa_{1-x}N$ alloys.

Under *n*-type conditions (large E_F values), the triply negatively charged aluminum vacancy V_{Al}^{3-} has the lowest formation energy. The behavior of the Al vacancy is similar to the case of the gallium vacancy in GaN. However, because of the larger band gap of AlN, the formation energy of V_{Al}^{3-} is significantly lower than V_{Ga}^{3-}. The defect level of V_{Al} lies close to the valence-band maximum, and is made up of states that reflect nitrogen-*p* (i.e., valence-band) character; we therefore expect that the corrections to the DFT-LDA band gap will not significantly affect the energetic position of this level, and consequently that the calculated formation energy of V_{Al}^{3-} will also be valid for all E_F values shown in Fig. 4.

Regarding the comparison between wurtzite and zinc-blende structures for V_N^{3+} and V_{Al}^{3-}, we found that the formation energies differ by only small amounts (by 0.01 and 0.13 eV, respectively). The defect geometries are also very similar, as discussed below. The main and important difference, as noted above, is that in a wurtzite structure the nitrogen vacancy induces an upper defect level below the CBM, which in the neutral charge state is occupied by a single electron, while in a zinc-blende structure this state is a resonance in the conduction band.

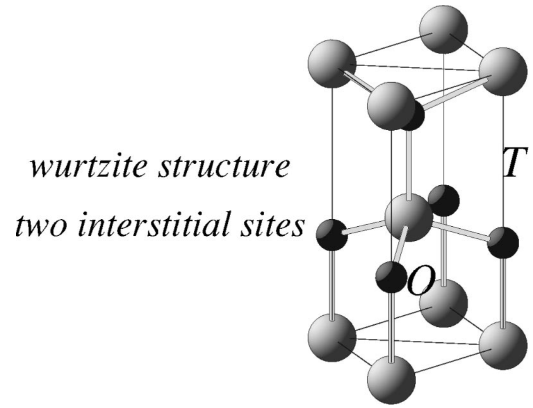

FIG. 5. Schematic representation of the wurtzite structure indicating the two high-symmetry interstitial positions *T* and *O*. Large gray and small dark spheres represent cations and anions, respectively.

2. Interstitials

The defect level induced by the aluminum interstitial, Al_i, lies high in the band gap, close to (or at) the conduction-band minimum. On emptying this state the formation energy is rapidly lowered as the Fermi level moves down. It can be seen that, for *p*-type conditions, the formation energy is very low, comparable to V_N^{3+}. In the $3+$ charge state the Al_i level has been emptied of all electrons; hence we anticipate that the calculated formation energy is accurate, using the same argument made above for the positive charge state of the nitrogen vacancy.

The equilibrium geometry for the Al-interstitial defect in zinc-blende AlN discussed above is that of the symmetric tetrahedral interstitial site, i.e., there is no tendency for the interstitial atom to assume a lower symmetry position. This is in contrast to the Al interstitial site in the wurtzite structure, which we also studied; in a wurtzite structure there are also two types of high-symmetry interstitial positions: (tetrahedral) *T* and (octahedral) *O* sites. The *T* site corresponds to the center of the line joining the closest nonbonded Al and N atoms along the *c* axis (see Fig. 5). It has two nearest neighbors (one cation and one anion) and six next-nearest neighbors (three cations and three anions). The *O* site is located at the center of the hexagonal channel, and has six nearest neighbors (three cations and three anions). For our wurtzite calculations, when using a 32-atom supercell, with six **k** points in the Brillouin zone and imposing no symmetry restrictions, we found that the *O* site is lower in energy than the *T* site by 1.53 eV, the formation energies for the *O* site being 14.30 and 10.76 eV for the neutral charge state under N- and Al-rich conditions, respectively. These values are more than 2.0 eV *higher* than for Al_i in the zinc-blende structure. The Al interstitial is thus not expected to be an important defect in wurtzite material. This difference is due to the different local atomic geometry of the interstitial sites in the two structures: in the zinc-blende structure the interstitial Al atom can be tetrahedrally bonded to *four* N atoms, but in wurtzite material, only three Al_i-N bonds are formed. A similar difference between wurtzite and zinc-blende struc-

tures was recently reported for interstitial beryllium impurities in GaN, and also explained in terms of a difference in coordination.[45]

In GaN it has been shown that a "(100) split-interstitial" configuration has the lowest formation energy[46] for an interstitial N atom. In this geometry two N atoms share the same substitutional site with a bond length similar to the N_2 dimer, and each N atom in the defect has two bonds to the surrounding cation atom instead of four. In AlN, we find that this N split-interstitial geometry, N_i^{sp}, is also energetically more favorable than the tetrahedrally coordinated interstitial site (see Fig. 4): in the neutral charge state its energy is lower by ≈ 2.0 eV. The (100) N split-interstitial defect introduces a pair of deep levels very close in energy which are occupied by three electrons. In Table I the percentage deviation in the bond length of the two N atoms sharing the same substitutional site is given with respect to that of the free N_2 molecule.

3. Antisites

Mattila *et al.*[11] identified the stability of an $EL2$ geometry for the N antisite in the negative charge states in both zinc-blende (ZB) and wurtzite (WZ) GaN and AlN. In this atomic configuration, there is a displacement of the nitrogen atom off the substitutional position along the [111](ZB) and [0001](WZ) directions. We have performed calculations for the N antisite in AlN investigating the stability of the $EL2$ geometry; we find that even in the neutral charge state the formation energy is lower than the substitutional antisite by 0.35 eV (see Fig. 4). In the neutral $EL2$ configuration there is a doubly occupied singlet state and above this level there are two deep unoccupied singlet states. We find that the singly negative charge state is not stable at any position of the Fermi level, therefore exhibiting a negative-U behavior. This was also found to be the case for GaN.[11] The displacement of the N atom along the [111] direction for the neutral charge state is 49% of the ideal Al-N nearest-neighbor distance, in agreement with Ref. 11. The displacements for the singly and doubly negative charge states are given in Table I. While the behavior of N_{Al}^{EL2} is very interesting, we doubt that this defect will play an important role in the electronic properties of AlN; indeed, Fig. 4 shows that aluminum vacancies are always lower in energy than nitrogen antisites in *n*-type AlN, and will therefore be the preferred compensating center.

Under N-rich conditions the Al antisite is a high energy defect. Under Al-rich conditions it has a low formation energy in the 4^+ charge state for strongly *p*-type material; it is however, higher than the V_N^{3+} and Al_i^{3+} defects and thus not expected to play an important role.

C. Comparison of GGA and LDA results

Figure 6 shows the comparison between formation energies obtained using the GGA vs the LDA. Only the lowest-energy defects and charge states (V_N^{3+}, Al_i^{3-}, and V_{Al}^{3-}) were included in this study. It can be seen that there is good qualitative agreement but that some quantitative deviations

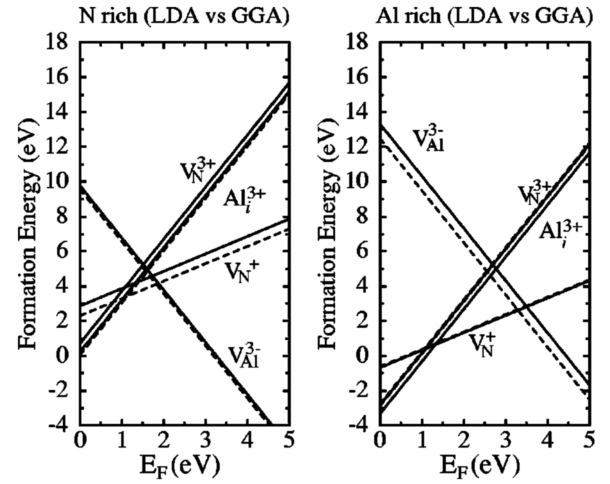

FIG. 6. Comparison of GGA (dashed lines) and LDA (solid lines) results for defect formation energies of various low-energy point defects in zinc-blende AlN. Formation energies are shown as a function of the Fermi level under nitrogen-rich (left panel) and aluminum-rich (right panel) conditions. $E_F = 0$ corresponds to the valence-band maximum.

occur. We were able to attribute the differences to two main effects: (i) Differences in the energies of the reservoirs [chemical potentials; see Eq. (1)] due to the LDA/GGA differences in cohesive energies, binding energies, and heats of formation. In particular, the cohesive energy of bulk Al is 0.65 eV smaller in the GGA than in the LDA; the binding energy of the N_2 molecule is 0.86 eV smaller (per N atom) in the GGA; and the magnitude of the heat of formation of bulk AlN is 0.35 eV smaller in the GGA.[31] We note that the GGA results for each of these systems are in better agreement with experiment (see Ref. 31). The LDA overbinding in the defect calculations is to some degree compensated due to the fact that the reservoir or reference systems also exhibit an overbinding; however, a complete cancellation does not occur. (ii) Differences in the band gap. The LDA and GGA band structures are extremely similar when calculated at the same lattice constant. For instance, at the *experimental* lattice constant the LDA and GGA band gaps differ by less than 0.02 eV. However, the point-defect calculations are carried out at the respective *theoretical lattice constants*, at which we find that the GGA band gap is 0.62 eV smaller than the LDA band gap.[31] The reduction in the band gap causes some of the defect-induced levels to lie at lower energies in the band gap, which could affect the calculated formation energy of defects for which these levels are occupied.

D. Atomic structure

In Table I we report the change in defect geometry with charge state for point defects in zinc-blende AlN. The displacement of the nearest-neighbor atoms of the defect with respect to the unrelaxed positions is given as a percentage of the ideal Al-N bond length. The nitrogen vacancy exhibits a strong dependence on the charge state: In the neutral charge state, the four surrounding Al atoms are almost unperturbed,

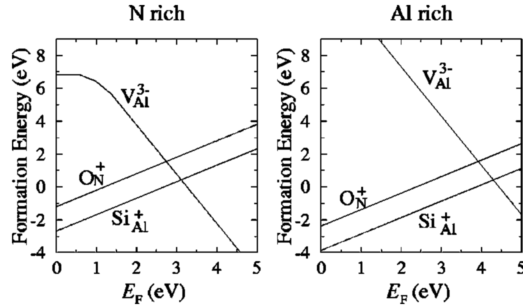

FIG. 7. Formation energies (LDA) of impurities and defects relevant for *n*-type AlN, as a function of the Fermi level under nitrogen-rich (left panel) and aluminum-rich (right panel) conditions. Oxygen and silicon are donor impurities, and the Al vacancy is the dominant compensating defect. $E_F=0$ corresponds to the valence-band maximum.

while, for an increasing positive charge state, the Al atoms move increasingly outwards. For the 3+ charge state, the displacement is 17%. (The corresponding GGA value is about 14%.) This can be compared to that of 19% for the same defect in GaN.[42] In a wurtzite structure, we find that the three equivalent nearest-neighbor Al atoms move outwards from the vacancy by 18% and the nonequivalent neighboring Al atom moves outwards by 27%.

In contrast, relaxations around the aluminum vacancy show very little dependence on the charge state, with roughly a 9–10 % outward breathing relaxation of the four neighboring N atoms. (The corresponding GGA value for V_{Al}^{3-} is 9%.) For V_{Al}^{3-} in wurtzite AlN the nearest-neighbor N atom along the *c* axis moves outward by $\approx 15\%$, and the three equivalent neighboring N atoms move outwards by 9%, similar to the relaxations in the zinc-blende structure.

The geometry of the aluminum interstitial, Al_i, also does not depend very strongly on the charge state, exhibiting a small *inward* movement of the neighboring N atoms of about 4%. The nitrogen split interstitial is the energetically favorable configuration for the N interstitial. It can be seen that for the 3+ charge states the distance between the two N atoms is only about 5% larger than in the N_2 molecule. When electrons are added to the defect level, the N-N distance is increased. Large outward relaxations are found for the aluminum antisite; this is due to the larger size of the Al atom as compared to the N atoms, and induces large internal strains, leading to rather high formation energies. The relaxations of Al_{N} become larger for increasing positive charge states, from 17% for $\mathrm{Al}_{\mathrm{N}}^{-}$ to 28% for $\mathrm{Al}_{\mathrm{N}}^{4+}$. The substitutional nitrogen antisite N_{Al} induces only very small displacements for the neutral charge state (1%), and increasingly larger outward displacements for *both* negative and positive charge states. We saw above that the energetically favorable configuration for N_{Al} is the so-called *EL*2 geometry. In this configuration the N atom has moved between 49% (neutral) and 39% (doubly negative) of the ideal Al-N distance along the [111] direction, thus forming shorter and stronger bonds with its three neighboring N atoms (as opposed to a tetrahedral bonding arrangement).

IV. IMPURITIES

A. Mg, O, and Si impurities

Figure 7 shows the calculated formation energy in zinc-blende AlN of the O and Si impurities, as well as V_{Al}^{3-}, as a function of E_{F} for both N- and Al-rich conditions. As found in earlier studies of O and Si in GaN (Ref. 44) and AlN,[11] oxygen substitutes on the N site and silicon substitutes on the cation site. The O and Si impurities introduce a singly occupied level which is a resonance in the conduction band. From Table I it can be seen that $\mathrm{O}_{\mathrm{N}}^{+}$ induces an outward expansion of the nearest four Al atoms of 3.8%, while for $\mathrm{Si}_{\mathrm{Al}}^{+}$ an inward relaxation of 5.0% of the neighboring N atoms occurs. The formation energies of O and Si in the positive charge state are very low in *p*-type material.

Magnesium in GaN has been shown to have the lowest formation energy when occupying the substitutional cation site.[47] We therefore assumed that for AlN it would also "prefer" the cation site and act as an acceptor. The Mg atom induces a large outward movement of the surrounding N atoms of 10.1% for Mg^0 and 9.4% for Mg^-. Figure 8 displays the calculated formation energy of the Mg impurity as well as of the dominant compensating defects in *p*-type AlN, namely, $V_{\mathrm{N}}^{3+/+}$ and Al_i^{3-}. The lowest-energy charge state of Mg changes from neutral to -1 at $E_F=0.4$ eV; this transition level corresponds to the acceptor ionization energy. This value can be compared to that calculated for GaN of ≈ 0.2 eV.[47] Experimentally, based on an analysis of temperature-dependent Hall data, Tanaka *et al.*[48] found the Mg activation energy to be 35 meV deeper in $\mathrm{Al}_{0.08}\mathrm{Ga}_{0.92}\mathrm{N}$ than in GaN. Assuming linearity, this would make the Mg acceptor in AlN 0.44 eV deeper than in GaN, in reasonable qualitative agreement with our computed result.

The low formation energies found in the present work for the triple donors, V_{N}^{3+} and Al_i^{3+}, under *p*-type conditions, indicate that these defects will compensate shallow acceptors (e.g., Mg), thus potentially interfering with attempts at *p*-type doping. In particular, the nitrogen vacancy has a lower formation energy in AlN than in GaN, indicating that compensation by nitrogen vacancies is therefore the likely cause of the decreased doping efficiency of Mg when the Al content is raised in $\mathrm{Al}_x\mathrm{Ga}_{1-x}\mathrm{N}$ alloys. The Al interstitial should not be a concern in wurtzite material, but is low in energy in zinc-blende AlN. Problems in achieving *p*-type $\mathrm{Al}_x\mathrm{Ga}_{1-x}\mathrm{N}$ for $x \geqslant 0.13$ have indeed been observed.[49] The low formation energy of the O and Si impurities in the positive charge state imply that either of these impurities, if present during *p*-type growth, will be readily incorporated and act as a compensating center.

We find that V_{Al}^{3-} has a sufficiently low formation energy to act as an effective compensating center for shallow donors (e.g., O and Si), inhibiting successful *n*-type doping. Severe problems in achieving *n*-type conductivity were reported in $\mathrm{Al}_x\mathrm{Ga}_{1-x}\mathrm{N}$ for $x \geqslant 0.4$; see, for example, Refs. 49–51. In Ref. 12 we proposed that the drop in *n*-type conductivity with increasing *x* can be attributed to two effects: (i) In the case of doping with oxygen (the most common unintentional donor), a *DX* transition occurs (in wurtzite material) which

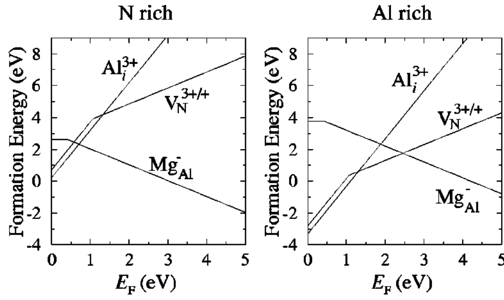

FIG. 8. Formation energies (LDA) of impurities and defects relevant for p-type AlN, as a function of the Fermi level under nitrogen-rich (left panel) and aluminum-rich (right panel) conditions. Magnesium is the acceptor impurity, and Al_i and V_N are the dominant compensating defects. $E_F=0$ corresponds to the valence-band maximum.

converts the shallow donor into a deep level;[43] the DX behavior of oxygen is not included in Fig. 7. (ii) Compensation by the cation vacancies (V_{Ga} or V_{Al}, triple acceptors) increases with alloy composition x.

B. Mg_nO_n complexes

We also performed calculations for complex formation between Mg and O in zinc-blende AlN, in particular MgO and Mg_2O_2. We consider Mg substituting on Al sites and O atoms on N sites. We calculate (i) the formation energy as given in Eq. (1) and (ii) the average binding energy, defined with respect to the separated impurities Mg_{Al}^- and O_N^+:

$$E^b(n\mathrm{Mg_{Al}};n\mathrm{O_N})=[-E^f(n\mathrm{Mg_{Al}};n\mathrm{O_N})+nE^f(\mathrm{Mg_{Al}^-})+nE^f(\mathrm{O_N^+})]/n, \tag{2}$$

where E^f are the formation energies of the defects indicated in the associated parentheses, and $n=1$ or 2.

The atomic structure of the MgO and Mg_2O_2 defects (at the ideal, unrelaxed positions) is shown in Fig. 9, where the binding energies are also given. The relaxed Mg-O bond lengths remain very similar in each Mg_nO_n defect, namely 2.09 Å for MgO and 2.08 Å for Mg_2O_2. These values are very close to those of crystalline MgO, where the bond length is 2.10 Å.[36] Compared to the N-Al nearest-neighbor distance (1.87 Å), the Mg-O bond lengths are about 11.5% longer. As discussed above, the Mg_{Al} defect is a shallow acceptor, and the O_N defect is a shallow donor. On forming the $Mg_{Al}O_N$ defect, we find that there are no longer any states in the band gap; there is an occupied defect state below the VBM and an unoccupied state above the CBM. The neutral MgO complex has a binding energy of 0.6 eV, as reported previously.[20] For the Mg_2O_2 defect, which forms an O-Mg-O-Mg zigzag structure, the binding energy per MgO unit is somewhat larger, namely, 0.8 eV. Again, in this case there are no states in the band gap. The stability of the com-

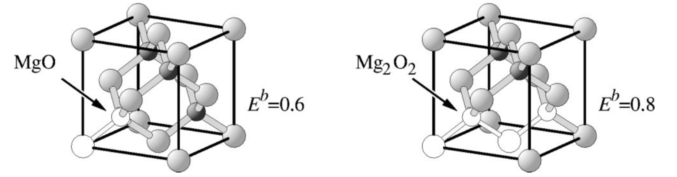

FIG. 9. Atomic geometry of MgO and Mg_2O_2 complexes in AlN. Large and small open circles represent Mg and O atoms, respectively, and large pale gray and small dark gray circles represent Al and N atoms, respectively. E^b is the binding energy (in eV) per MgO pair.

plexes can be understood as reflecting the larger bond strength of Mg-O as compared to Mg-N: the heat of formation of crystalline MgO is -6.16 eV, and for MgO_2 the value is -6.46 eV, as compared to -4.81 eV for Mg_3N_2.[36] The formation energies of the MgO and Mg_2O_2 defects are 0.92 and 1.67 eV, respectively. These quantities are independent of E_F, since the complexes are neutral, and are the same for N- and Al-rich conditions due to the assumed chemical potentials described above. Thus, on thermodynamic grounds, due to its relatively high formation energy, we conclude that the Mg_2O_2 complex is unlikely to be present in any significant quantities. MgO pairs, however, may be more abundant and could play a role in the compensation of acceptor doping with Mg if oxygen is present as a contaminant.

V. CONCLUSION

We have performed first-principles calculations for native point defects and selected impurities in AlN. The triply positively charged nitrogen vacancy (and the triply positively charged aluminum interstitial, in zinc-blende AlN) have the lowest formation energies in p-type material, and in n-type material the triply negatively charged aluminum vacancy has the lowest formation energy. Due to the low formation energies, the triple donors V_N^{3+} and Al_i^{3+} may act as compensating centers when trying to achieve p-type doping (e.g., with Mg). If oxygen contaminants are present in the material, then substitutional $Mg_{Al}O_N$ pairs may also contribute to the compensation. In n-type material, V_{Al}^{3-} may act as a compensating center, thus limiting the electron concentration provided by Si and O impurities which we find are shallow donors. The formation energy of the nitrogen vacancy is high in n-type AlN, indicating that this defect is not expected to occur in high concentrations. V_N^{2+} is found to be unstable; thus there is a negative-U effect between V_N^+ and V_N^{3+}. For the nitrogen antisite we find that the $EL2$ configuration is the stable one for the neutral and negative charge states, where the singly negative charge state is found to be unstable, so that there is also a negative-U effect between $N_{Al}^{EL,0}$ and $N_{Al}^{EL,2-}$. This defect, however, has a high formation energy, indicating that it will not be present in high concentrations. For the N interstitial, we identified the stability and energetic

preference for a (100) split interstitial configuration. Again it is a high-energy defect. We find that the nature of the nitrogen vacancy is different in the zinc-blende and wurtzite structures in that the higher lying defect-induced level is a resonance in the conduction band in a zinc-blende structure but lies well below the conduction-band edge in a wurtzite structure. The nitrogen vacancy is thus a shallow donor in a zinc-blende structure, but a deep donor in wurtzite AlN. From comparison of the GGA and LDA results, for the systems investigated, we find some quantitative differences but *qualitative* agreement.

ACKNOWLEDGMENTS

This work was supported in part by the Air Force Office of Scientific Research, Contract No. F4920-00-C-0019. C.S. gratefully acknowledges support from the DFG (Deutsche Forschungsgemeinschaft).

[1] H. Morkoç, S. Strite, G. B. Gao, M. E. Lin, B. Sverdlov, and M. Burns, J. Appl. Phys. **76**, 1363 (1994), and references therein.

[2] F. A. Ponce and D. P. Bour, Nature (London) **386**, 351 (1997), and references therein.

[3] S. Nakamura, Solid State Commun. **102**, 237 (1997), and references therein.

[4] S. Nakamura, T. Mukai, and M. Senoh, Appl. Phys. Lett. **64**, 1687 (1994); S. Nakamura, M. Senoh, N. Iwasa, S. Nagahama, T. Yamada, and T. Makai, Jpn. J. Appl. Phys. **34**, L1332 (1995).

[5] S. Nakamura, M. Senoh, S. Nagahama, N. Iwasa, T. Yamada, T. Matsushita, H. Kiyaku, and Y. Sugimoto, Jpn. J. Appl. Phys. **35**, L74 (1996); S. Nakamura, in *III-V Nitrides*, edited by F. A. Ponce, T. V. Moustakas, I. Akasaui, and B. A. Monemar, Mater. Res. Soc. Symp. Proc. No. 449 (Materials Research Society, Pittsburgh, 1996), p. L74.

[6] K. Itaya, M. Onomura, J. Nishio, L. Sugiura, S. Saito, M. Suzuki, J. Rennie, S. Nunoue, M. Yamamoto, H. Fujimoto, Y. Kokubun, Y. Ohba, G. Hatakoshi, and M. Ishikawa, Jpn. J. Appl. Phys. **35**, L1317 (1996).

[7] U. Kaufmann, M. Kunzer, M. Maier, H. Obloh, A. Ramakrishnan, B. Santic, and P. Schlotter, Appl. Phys. Lett. **72**, 1326 (1998).

[8] J. I. Pankove, J. T. Torvik, C.-H. Qiu, I. Grzegory, S. Porowski, P. Quigley, and B. Martin, Appl. Phys. Lett. **74**, 416 (1999).

[9] D. W. Jenkins and J. D. Dow, Phys. Rev. B **39**, 3317 (1989).

[10] T. Mattila and R. M. Nieminen, Phys. Rev. B **54**, 16 676 (1996); **55**, 9571 (1997).

[11] T. Mattila, A. P. Seitsonen, and R. M. Nieminen, Phys. Rev. B **54**, 1474 (1996).

[12] C. Stampfl and C. G. Van de Walle, Appl. Phys. Lett. **72**, 459 (1998).

[13] C. Stampfl and C. G. Van de Walle, in *Nitride Semiconductors*, edited by F. A. Ponce, S. P. Den Baars, B. K. Meyer, S. Nakamura, and S. Strite, MRS Symposia Proceedings No. 482 (Materials Research Society, Pittsburgh, 1998), p. 905.

[14] A. Fara, F. Bernardini, and V. Fiorentini, J. Appl. Phys. **85**, 2001 (1999).

[15] P. Boguslawski and J. Bernholc, Phys. Rev. B **56**, 9496 (1997).

[16] C. H. Park and D. J. Chadi, Phys. Rev. B **55**, 12 995 (1997).

[17] I. Gorczyca, A. Svane, and N. E. Christensen, Solid State Commun. **101**, 747 (1997).

[18] I. Gorczyca, A. Svane, and N. E. Christensen, Phys. Rev. B **60**, 8147 (1999); Acta Phys. Pol. A **92**, 785 (1997).

[19] I. Gorczyca, A. Svane, and N. E. Christensen, Phys. Rev. B **61**, 7494 (2000).

[20] C. G. Van de Walle, C. Stampfl, and J. Neugebauer, J. Cryst. Growth **189/190**, 505 (1998).

[21] M. Bockstedte, A. Kley, J. Neugebauer, and M. Scheffler, Comput. Phys. Commun. **107**, 187 (1997).

[22] D. M. Ceperley and B. I. Alder, Phys. Rev. Lett. **45**, 566 (1980); P. Perdew and A. Zunger, Phys. Rev. B **23**, 5048 (1981).

[23] J. P. Perdew, J. A. Chevary, S. H. Vosko, K. A. Jackson, M. R. Pederson, D. J. Singh, and C. Fiolhais, Phys. Rev. B **46**, 6671 (1992).

[24] The GGA has been found to improve the description of total energies, ionization energies, and electron affinities of atoms, atomization energies of molecules, and some solid state properties (Ref. 23), in addition to the adsorption energies [see, e.g., P. H. T. Philipsen, G. te Velde, and E. J. Baerands, Chem. Phys. Lett. **226**, 583 (1994); P. Hu, D. A. King, S. Crampin, M.-H. Lee, and M. C. Payne, *ibid.* **230**, 501 (1994)]; and reaction energies [see, e.g., D. Porezag and M. R. Pederson, J. Chem. Phys. **102**, 9345 (1995); J. Baker, M. Muir, and J. Andzelm, *ibid.* **102**, 2063 (1995)]; Furthermore, the GGA has been shown to be crucial in obtaining activation energy barriers consistent with experiment for H_2 dissociation [see, e.g., B. Hammer, K. W. Jacobsen, and J. K. Norskov, Phys. Rev. Lett. **70**, 3971 (1993); B. Hammer, M. Scheffler, K. W. Jarcobsen, and J. K. Norskov, *ibid.* **73**, 1400 (1994)]; Also the relative stability of structural phases appear to be better described for magnetic [see, e.g., T. C. Leung, C. T. Chan, and B. N. Harmon, Phys. Rev. B **44**, 2923 (1991)] and nonmagnetic systems [see, e.g., N. Moll, M. Bockstedte, M. Fuchs, E. Pehlke, and M. Scheffler, *ibid.* **52**, 2550 (1995); D. R. Hamann, Phys. Rev. Lett. **76**, 660 (1996); We refer to Ref. 30 for a detailed discussion].

[25] *Properties of Group III-Nitrides*, edited by J. H. Edgar, EMIS Datareviews Series (INSPEC, London, 1994).

[26] H. J. Monkhorst and J. D. Pack, Phys. Rev. B **13**, 5188 (1976).

[27] S. L. Cunningham, Phys. Rev. B **10**, 4988 (1974).

[28] N. Troullier and J. L. Martins, Phys. Rev. B **43**, 1993 (1991).

[29] M. Fuchs and M. Scheffler, Comput. Phys. Commun. **119**, 67 (1999).

[30] M. Fuchs and M. Scheffler, Phys. Rev. B **57**, 2134 (1998).

[31] C. Stampfl and C. G. Van de Walle, Phys. Rev. B **59**, 5521 (1999).

[32] C. Stampfl and C. G. Van de Walle, Phys. Rev. B **57**, R15 052 (1998).

[33] C. Stampfl, C. G. Van de Walle, D. Vogel, P. Krüger, and J. Pollmann, Phys. Rev. B **61**, R7846 (2000).

[34] D. B. Laks, C. G. Van de Walle, P. E. Blöchl, and S. T. Pantelides, Phys. Rev. B **45**, 10 965 (1992).

[35] A. Garćia and J. E. Northrup, Phys. Rev. Lett. **74**, 1131 (1995).

[36] *Handbook of Chemistry and Physics*, 76th ed., edited by D. R. Lide (CRC Press, Boca Raton, FL, 1995).

[37] J. P. Perdew and M. Levy, Phys. Rev. Lett. **51**, 1884 (1983); L. J. Sham and M. Schlüter, *ibid.* **51**, 1888 (1983).
[38] A. Rubio, J. L. Corkhill, M. L. Cohen, E. Shirley, and S. G. Louie, Phys. Rev. B **48**, 11 810 (1993).
[39] S. B. Zhang and D. J. Chadi, Phys. Rev. B **42**, 7174 (1990).
[40] D. Vogel, P. Krüger, and J. Pollmann, Phys. Rev. B **54**, 5495 (1996).
[41] C. Stampfl, C. G. Van de Walle, M. Fuchs, D. Vogel, P. Krüger, and J. Pollmann (unpublished).
[42] J. Neugebauer and C. G. Van de Walle, Festköerperprobleme **35**, 25 (1996).
[43] C. G. Van de Walle, Phys. Rev. B **57**, R2033 (1998).
[44] J. Neugebauer and C. G. Van de Walle, in *22nd International Conference on the Physics of Semiconductors*, *Vancouver, Canada 1994* (World Scientific, Singapore 1995), p. 2327.
[45] C. G. Van de Walle, S. Limpijumnong, and J. Neugebauer, Phys. Rev. B **63**, 245205 (2001).
[46] J. Neugebauer and C. G. Van de Walle, Phys. Rev. B **50**, 8067 (1994).
[47] J. Neugebauer and C. G. Van de Walle, Appl. Phys. Lett. **68**, 1829 (1996).
[48] T. Tanaka, A. Watanabe, H. Amano, Y. Kobayashi, I. Akasaki, S. Yamazaki, and M. Koike, Appl. Phys. Lett. **65**, 593 (1994).
[49] M. D. Bremser, W. G. Perry, T. Zheleva, N. V. Edwards, O. H. Nam, N. Parikh, D. E. Aspnes, and R. F. Davis, MRS Internet J. Nitride Semicond. Res. **1**, 8 (1998).
[50] H. G. Lee, M. Gershenzon, and B. L. Goldenberg, J. Electron. Mater. **20**, 621 (1991).
[51] X. Zhang, P. Kung, A. Saxler, D. Walker, T. C. Wang, and M. Razeghi, Appl. Phys. Lett. **67**, 1745 (1995).